Chemical Geology 600 (2022) 120865

Contents lists available at ScienceDirect

Chemical Geology

journal homepage: www.elsevier.com/locate/chemgeo

Evaluation of environmental radioactivity in soils around a coal burning power plant and a coal mining area in Barapukuria, Bangladesh: Radiological risks assessment

Md. Ahosan Habib [a,c], Rahat Khan [b,*], Khamphe Phoungthong [a,*]

[a] Environmental Assessment and Technology for Hazardous Waste Management Research Center, Faculty of Environmental Management, Prince of Songkla University, Songkhla 90112, Thailand
[b] Institute of Nuclear Science and Technology, Bangladesh Atomic Energy Commission, Savar, Dhaka 1349, Bangladesh
[c] Geological Survey of Bangladesh, 153 Pioneer Road, Seghunbaghicha, Dhaka 1000, Bangladesh

ARTICLE INFO

Editor: Claudia Romano

Keywords:
Barapukuria, Bangladesh
Coal-based industrial activities
Soils around coal-industries
Major oxides
Distribution of NORMs
Radiological risks

ABSTRACT

To study the distributions and potential dispersions of naturally occurring radioactive materials (NORMs: ^{226}Ra, ^{232}Th, and ^{40}K) from coal-based activities (Barapukuria, Bangladesh), we studied a suite of systematically collected surface and sub-surface soil samples by X-ray fluorescence and high purity germanium detector based γ-spectroscopy. The average (range) radioactivities of ^{226}Ra, ^{232}Th, and ^{40}K in the studied soil samples were 80.6 (33.0–118.0), 104.4 (43.0–182.0), and 508.1 (318.3–743.4) Bq.kg^{-1}, respectively, which are significantly higher than the corresponding world average value. No significant fractionations of NORMs were observed between the surface and sub-surface soils, except for ^{232}Th. Along with the anthropogenic origin, several geochemical processes (e.g., weathering, mineralogical dissolution/precipitation, alteration, leaching, differential solubility mediated geochemical mobility etc.) play significant role in NORM distributions. Major-oxide abundances, indices-based calculations, and correlation studies on the measured parameters revealed the natural processes (e.g., geochemical mobility, mineralogical distributions, water logging based differential solubility) responsible for NORM distributions. In terms of mean radium equivalent activity, internal hazard index, and total annual effective dose values, the studied area possesses trivial radiological risks, whereas the values of internal absorbed gamma dose and excess lifetime cancer risk demonstrate significant health hazards. Considering the adverse radiological risks originating from coal-based industrial activities and the long half-lives of NORMs, the present scenario will potentially be deteriorated.

1. Introduction

The exposure of humans to external gamma ray from geo-resources is a continuing and inescapable feature of living beings in the world given that natural radionuclides are ubiquitous and widely distributed at different trace levels in various geological samples (Bunzl et al., 1984; Siegel and Bryan, 2014; Alazemi et al., 2016; Aközcan et al., 2018; Ugbede et al., 2021). Coal-fuel is combusted for nearly 38% of power production throughout the world. From 2017 to 2018, the global utilization of coal to generate electricity increased by 3%, and it was driven by the increased use in numerous developing countries, such as Bangladesh, China, India, and Southeast Asia (Habib and Khan, 2021). Inherently, feeding coals and associated tailings and wastes commonly contain a significant fraction of various (in)organic constituents, including trace quantities of naturally occurring radioactive materials (NORMs e.g., ^{226}Ra, ^{232}Th, and ^{40}K), which are potentially harmful and radiotoxic (Vuković et al., 1996; Dragović et al., 2013, Galhardi et al., 2017; Turhan, 2020). These materials can result in significant additional contributions to the radioactive burden of the ambient environment and people living and working in the immediate vicinity of coal mine and coal-based power stations (CMPSs) (Noli et al., 2017; Khan et al., 2018, 2021a, 2021b; Habib et al., 2019a, 2019b). NORMs are commonly present at different trace levels in all geo-materials and represent the main external source of radiation to the people (UNSCEAR, 2010). Soil contamination with NORMs draws great attention worldwide due to its possible threat to food safety, living beings, and its detrimental effects on the surroundings.

NORMs can easily be released from coal-related products in diverse

* Corresponding authors.
E-mail addresses: rahatkhan.baec@gamil.com (R. Khan), khamphe.p@psu.ac.th (K. Phoungthong).

https://doi.org/10.1016/j.chemgeo.2022.120865
Received 31 December 2021; Received in revised form 21 February 2022; Accepted 9 April 2022
Available online 13 April 2022

means and pathways (e.g., emissions, effluents, and leachates from CMPSs) with substantial proportions penetrating the ambient environment (Sengupta and Agrahari, 2017). Moreover, these excessive NORMs can infiltrate, adsorb, and excessively accumulate in soils and result in the increased levels of these pollutants and their transfer from soil to water sources and food chain (Skoko et al., 2017), which ultimately promote human exposure to gamma radiation and consequently harm public health through the food chain (Skoko et al., 2017; Duong et al., 2021). Once the specific activities involving NORMs exceed the corresponding desirable limits, environmental contamination becomes inevitable. The location, extent, and severity of exposure to gamma radiation can be distorted by the differential migration of transportable proportions of NORMs to the environment. Soil serves as the primary reservoir for NORM accumulation in the terrestrial environment (Dai et al., 2007). Moreover, soil is one of the most important environmental backgrounds because it provides water and nutrients for plant production (Kabata-Pendias, 2010). Thus, the identification, quantification, characterization of the activity level, effective dose consequences, unfavorable impacts, potential radiological risk and distribution, accumulation, migration, and source of NORMs in soils are crucial to ascertain possible changes in environmental radioactivity due to such activities (Baeza et al., 2012; Ćujić et al., 2015). Moreover, quality standards on a national and regional level must be established to form and enforce regulations on NORM discharges.

A rapidly growing research interest that receives global attention focuses on determining the radioactivity in soil along with their radiological risks for the establishment of national, regional, and global data banks despite the inevitability of radioactivity on earth. Previous studies demonstrated insignificant effects of NORMs from CMPS on the soil (Rosner et al., 1984; Vuković et al., 1996; Tsikritzis, 2004; Charro et al., 2013a, 2013b; Papaefthymiou et al., 2013; Lu et al., 2013; Suhana and Rashid, 2016; Habib et al., 2019a), whereas other research identified the profound impacts of NORMs on soil quality (Bem et al., 2002; Flues et al., 2002; Papp et al., 2002; Dai et al., 2007; Amin et al., 2013; Ćujić et al., 2015; Liu et al., 2015; Medunić et al., 2016; Parial et al., 2016; Gören et al., 2017; Zhang, 2017; Dhingra et al., 2020; and the references therein). However, an uncertainty surrounds the degree of radiological influence and radioactivity impact on human health due to the operation of CMPSs. Radiological study on soils around the Barapukuria coal-based power plant (Bangladesh), which was confined to a 3 km perimeter, demonstrated 2–4 times elevated concentrations of NORMs than the recommended limits of the United Nations Scientific Committee on the Effects of Atomic Radiation (UNSCEAR, 2000, 2010) (Habib et al., 2019b). Thus, considering the radiological risks, studies should determine the level of NORMs and their influence on soils and human health around CMPSs. In this endeavor, the radiological doses and associated risk were computed for the population residing up to a distance of 15 km from a CMPS. The measurement and characterization of NORM distributions in soils can offer useful information not only about the levels, spatial variation, sources, transport mechanisms, and environmental fate but also the evaluation of radio-environmental risks and the control of radioactivity (Çayır et al., 2012; Tanić et al., 2016).

The geochemical characterization of soils was extensively considered to decipher source rock geochemistry, provenance, and source-area weathering. These factors greatly influence the sink material composition. The provenance analysis enabled us to detect the source areas of the samples and establish the linkage between the province and depositional areas through specific geological processes (Carvalho et al., 2011; Begum et al., 2021a, 2021b). The abundances of specific major and radioactive elements were less altered by diverse geological processes, as determined by the examination of geochemical characteristics of soils. The levels of radioactivity were generally associated with the types of rocks and their geochemistry, sediments, or soils from which the samples were derived (Begum et al., 2021a, 2021b). However, potential interactions between major and radioactive elements along with their influences and function of minerals on the variability of the activity, genesis, environmental fate, and behavior of NORMs in soils have not been explored thus far in and around the Barapukuria area (Dragović et al., 2008; Suresh et al., 2011; Churchman and Lowe, 2012; Ćujić et al., 2015; Guagliardi et al., 2016; Ribeiro et al., 2018). Furthermore, coal-fuel will play an important role to meet the growing energy needs of Bangladesh in the coming years (Habib et al., 2020). At present, the established electricity production capacity of the country is above 12,780 MW, which is planned to increase to 39,000 MW by 2030, and a major portion of it will be sourced from coals (Habib and Khan, 2021).

This study dealt with the evaluation of the influences of a CMPS on the activity levels of NORMs and major elemental chemistry of soils in their immediate proximity with deciphering information regarding provenance and weathering conditions. The principal focuses of the current research are to (i) quantify the activity levels, (ii) compute the radiological dose consequences of radiation received for the nearby population, (iii) evaluate the radiological distribution and risk maps for the studied area, (iv) evaluate their mutual relationships between major oxides and NORMs, (v) determine potential source rocks of the analyzed soils and weathering, and (vi) evaluate the radiological hazards. The outcomes of this study will update existing scientific knowledge for further research, pollution control, and environmental management and will be treated as valuable reference information for future endeavors. This study lays the groundwork for future research related to the environmental and health concerns of waste disposal and accidental release of wastes containing increased concentrations of NORMs to the ambient environment. Furthermore, monitoring data on NORM distribution in and around the CMPS can help policymakers to enforce regulations on NORMs discharged from CMPSs.

2. Materials and analytical methods

2.1. Geomorphology, geology, pedology, and profile of the study area

The Barapukuria CMPS is situated at 25°33′36″ N, 88°56′45.6″ E in a humid subtropical region in Dinajpur district in the northwestern region of Bangladesh (Fig. 1). The surrounding areas are extensively used for agriculture, mainly in paddies with double/triple crops. The population density in the area is 770 km^{-2} (Population Census of Bangladesh, 2011). The average annual rainfall varies from 1104 mm to 2985 mm (from 1991 to 2015), of which 85% falls from May to September, and the relative humidity is 80% to 90%. The prevailing dominant local wind direction is from east to west (40%), followed by west to east (25%) and north-east (18%). Wind speeds rarely exceed 8 $m.s^{-1}$. The wind changes its directions depending on the seasons.

Tectonically, the area is situated within the Rangpur Saddle (Dinajpur Shield) of the Stable Shelf Zone, northwestern Bengal Basin, Bangladesh (Habib et al., 2019b). Physiographically, it is located at the northern fringe of a Pleistocene terrace (level Barind clay residuum) and close to the Young Tista floodplain, in an alluvial–fluvial floodplain system. Barind clay is mainly composed of red, reddish brown, brownish gray and gray mottled sandy clay, clayey silt, or silty clay, whereas Tista floodplain consists of olive gray, dark gray to gray clayey silt and silty clay loam soil. Iron–manganese oxide nodules are common in the upper part. The area is well-drained by a number of rivers, such as Atrai, little Jamuna, Karatoya, Banglai, Jabuneswari, Kala, Kharkhari, Tilai, Chirnai etc., flowing from north to south. Pedologically, the area comprises gray floodplain (dominant) and non-calcareous brown floodplain soils, deep red-brown terrace soils, and gray terrace soils (Habib et al., 2019a). Topographically, it is nearly a level board terrace/medium high-land type. Amnura, Belabo, Noadda, and Jagdal are the local soil series types. According to United States Department of Agriculture taxonomy, the soil is Aerie Haplaquept. The mean grain distribution of sand, silt, and clay are 7.8%, 75.1%, and 17.2%, respectively. The soil pH ranges from 4.0 to 6.3 with an average of 5.4 (Habib et al., 2019b).

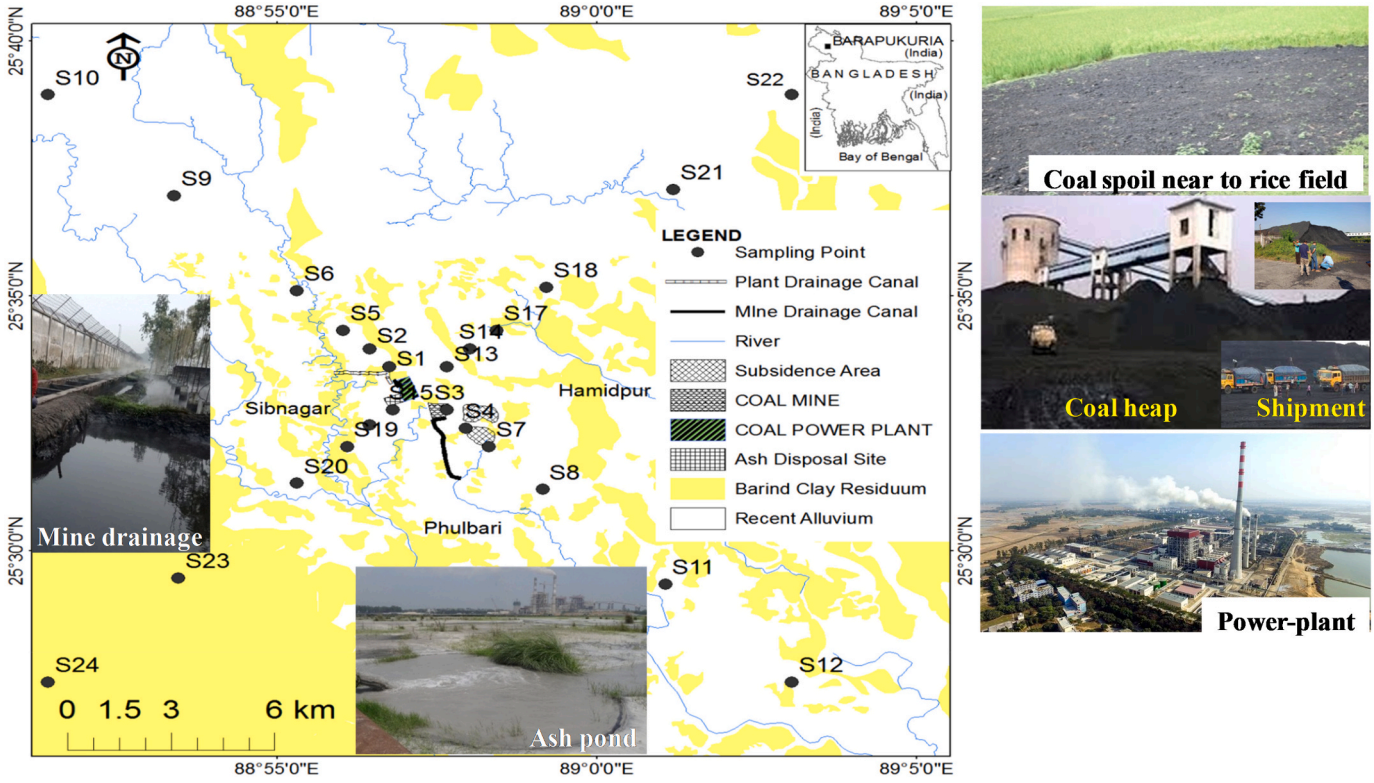

Fig. 1. Map showing the location of sampling sites in the surveyed area (Barapukuria, Bangladesh) with photographs of major contributing possible sources of NORMs to the surroundings.

2.2. Sampling strategy and sample preparation

To provide a satisfactory radio-environmental representation of the study area, a total of 48 samples of (un)cultivated soils (predominantly silty clay to clayey silt loam) were taken in the Barapukuria power-plant, coalfield and settlement areas applying the 'systematic random sampling' procedure (IAEA, 2004; ASTM C 998–83, 1983; Dragović et al., 2013; Ćujić et al., 2015, 2016; Liu et al., 2015) at a certain interval up to 15 km distance from the CMPS surroundings with a corer using cylindrical sampling units made of steel from 24 locations (predefined sample code S1-S24) to the NW, SE, SW, and NE (Tanić et al., 2018) (topsoil, $n = 24$, 0–15 cm depth: plough layer, A-horizon; sub-soil, n = 24, 15–30 cm, depth: undisturbed layer, B-horizon) in order to determine whether the NORMs concentrated mostly on the surface or whether they moved/mixed with deeper layers. From each site, 2–3 subsamples were collected from a 1×1 m^2 area up to a depth of interest (Fig. 1) in order to assess soil NORMs pollution. The sampling sites were selected in such a way to cover the entire vicinity of the power-station. The locations for sampling were selected so that they proportionately represent all geomorphologic units, spatial, lithological, geomorphological, pedological variability; various land uses, wind directions, height of the chimney, proximity to highly contaminated areas, and behind and in front of CMPS along the most frequent wind direction in the region. A sampling depth of 0 of 15 cm was selected because the study was primarily focused on human exposure risks from ingestion, inhalation, and dermal contact of these surface soils. Moreover, these topsoils are more chemically and biologically more active than underlying soils. Sites far away (15 km) from the power-station area are believed to be less affected by pollution due to combustion and other associated activities. After sampling, all samples were immediately packed in bags with proper labeling, carefully transported back to the laboratory and stored at low temperature before subsequent analysis. In all studies, the soil subsamples were blended thoroughly to have a composite replicate sample. All samples were then air-dried at room temperature and ground into powder by agate mortar and pestle to pass through a 2-mm sieve followed by 70 °C oven drying to have constant weight.

2.3. Sample analysis

Organic carbon was determined by a standard method, and the values were converted to organic matter (OM) content multiplied by a factor of 1.724 (Tsikritzis, 2004; Charro et al., 2013 a, b; Habib et al., 2019b). On the other hand, the levels of major elements (eight oxides: SiO_2, Al_2O_3, Fe_2O_3, MgO, CaO, Na_2O, K_2O, and TiO_2) of the soil samples were examined by following the identical procedure of Goto and Tatsumi (1994, 1996) using X-ray fluorescence (XRF; PW 2400, Philips, The Netherlands) through quantitative analyses at the Office of Scientific Instrument and Testing, Prince of Songkla University, Thailand. The prepared powdered samples (3 g) were placed in a porcelain crucible, mixed with a binder (wax: sample, 1:3), and shaken for 2 h. The resulting mixture was spooned into an aluminum cap (30 mm) that was sandwiched between two tungsten carbide pellets with a hydraulic press and then pressure was removed gradually. Finally, the pellet was determined by XRF. The Standard Reference Materials (SRMs) preferred in the current study were Stream Sediments (JSD 1, JSD 2 and JSD 3) sourced from the Geological Survey of Japan for the construction of calibration curves in order to verify sensitivity, repeatability, and reproducibility of the measurements and to check the quality assurance and control. The obtained experimental uncertainties were of ~2%. The calibration curve for individual major constituents were constructed based on the K X-ray and L X-ray intensities computed for the respective constituents contain the SRMs. The precision and accuracy of the measurement were welcomed only when the estimated Relative Standard Deviations (RSD) were of <5%, according to the results of duplicate analyses of the measured soils and the SRMs. The precision of major element abundances (<5%) was proved by analysis of the SRMs during operation. To verify the precision of the measurement, two randomly selected samples were measured three times and the estimated RSDs

were found at 3 to 5%. The accuracy of measurement was calculated by comparing the obtained results of SRM against the certified values and the percentage of recovery was within 94–106%.

The NORMs in soil samples were determined by following the identical procedure reported by our previous studies (Habib et al., 2019a, 2019b; Khan et al., 2019a, 2019b, 2019c, Khan et al., 2021a, 2021b). Samples were hermetically filled in cylindrical container to prevent the loss of the NORMs in the form of gaseous radon (Rn) and stored at least for 4 weeks to attain the secular equilibrium. Prepared samples were then measured by γ-ray spectrometer with low background HPGe detector (GEM 30–70, ORTEC, p-type, co-axial) for ~90,000 s. Similarly, a procedure blank sample was also measured for 3 days. Energy and efficiency calibration of γ-spectrometer were conducted by using a set of standard sources (^{109}Cd: 88.03 keV; ^{57}Co: 122.06, 136.47 keV; ^{139}Ce: 165.85 keV; ^{51}Cr: 320.08 keV; ^{85}Sr: 513.99 keV; ^{137}Cs: 661.65 keV; ^{54}Mn: 834.83 keV; ^{88}Y: 898.02 keV; ^{60}Co: 1173.24, 1332.5 keV; ^{88}Y: 1836.01 keV) those consist of radionuclides with known radioactivity and emits from low to high energy γ-ray manufactured by Japan Radioisotope Association. Activity concentration of NORM was calculated by considering net count, counting efficiency and emission rate of certain radionuclides and weight of sample, as in the following Eqs. (1) and (2):

$$A = \frac{Cps_{sample} - Cps_{BG}}{\varepsilon \times I_{\gamma}} \quad (1)$$

$$AC = \frac{A}{w} \quad (2)$$

where, A is activity (Bq), AC is activity concentration (Bq.kg^{-1}), Cps_{sample} is counts per second of sample (s^{-1}), Cps_{BG} is counts per second of background (s^{-1}), ε is counting efficiency of the HPGe detector, I_{γ} is intensity of γ-ray and w is sample weight (kg).

The NORMs of concern in this measurement are long half-lived radionuclides including ^{226}Ra and ^{232}Th and were estimated based on the activity concentration of γ-rays of their progenies in samples, except for ^{40}K that was measured directly. In ^{232}Th decay series, ^{228}Ac, ^{208}Tl, ^{212}Pb, ^{212}Bi were used to estimate ^{232}Th (L'Annunziata, 2003). In ^{238}U decay series, ^{214}Pb and ^{214}Bi were used to estimate ^{226}Ra. Reference materials (IAEA-RM-Soil-6 and IAEA-RM-375) were measured similarly to ensure the data quality. The specific activity levels (Bq.kg^{-1}) of U and Th were transformed to mass concentrations (ppm) divided by factors of 12.35 and 4.06, respectively.

2.4. Dosimetric calculations

The most commonly used radiological hazard parameters used in this study were radium equivalent activity (Ra_{eq}) (Beretka and Mathew, 1985), internal hazard index (H_{in}), internal absorbed gamma dose (GAD_i), total annual effective dose (AED_T), and excess lifetime cancer risk (ELCR: ICRP (International Commission on Radiological Protection), 1990), which were respectively estimated by the following equations (UNSCEAR, 2000):

$$Ra_{eq} = \left(\frac{A_{Ra}}{370} + \frac{A_{Th}}{259} + \frac{A_k}{4810}\right) \times 370 \quad (1)$$

$$H_{in} = \frac{A_{Ra}}{185} + \frac{A_{Th}}{259} + \frac{A_k}{4810} \quad (2)$$

$$GAD_i = (0.462A_{Ra} + 0.604A_{Th} + 0.0417A_K) \times 1.2 \quad (3)$$

$$AED_T = GAD_i \times 8760 \times 0.2 \times 0.7 \times 10^{-6} \quad (4)$$

$$ELCR = AED_T \times A_{lf} \times R_f \quad (5)$$

where the activity concentrations of ^{226}Ra, ^{232}Th, and ^{40}K (Bq.kg^{-1}) are expressed by A_{Ra}, A_{Th}, and A_K, respectively. A_{lf} represents the average lifetime (70 yr), and R_f denotes the cancer risk factor (0.5×10^{-4} Sv^{-1}) for public exposure.

2.5. Data presentation and statistical approaches

Spatial distribution maps of NORMs and corresponding radiological risks were prepared by ArcGIS software (Version 10.3, ESRI, California USA). Using SPSS software (Version-20, IBM-Corporation, Armonk, NY, USA), multivariate statistical analyses (Hasan et al., 2022; Ahsan et al., 2019; Rahman et al., 2022) were carried out on the measured parameters to determine the existing inter-relations and the spatial distribution of radionuclides.

3. Results and discussions

3.1. Organic materials and major oxides in soil samples

In this work, the content of OM ranged from 0.5% to 9.5% with an average of 1.5%. Table 1 presents the concentrations of major elemental constituents in soil samples in and around the Barapukuria CMPS. The average (range) concentrations of SiO_2, Al_2O_3, Fe_2O_3, TiO_2, Na_2O, and K_2O in soils were 65.8 (56.4–78.9), 12.8 (8.2–18.6), 3.6 (1.2–6.8), 0.91 (0.50-4.1), 0.34 (0.13–1.1), and 2.0 (1.2–2.9) wt%, respectively. Compared with world soil (WS: Bowen, 1979), the Ti and K contents were relatively higher (Fig. S1), whereas other major elements were depleted in the samples. Upper continental crust (UCC: Rudnick and Gao, 2014), WS, and world shale (WSH: Bowen, 1979)-normalized major oxides contents of the investigated samples were < 1, which indicated their loss from source rocks during diverse natural processes compared with the background composition, except for Ti (for UCC, WS, and WSH), K (for WS), and Si (for WSH) (Fig. S1). The major oxides with other trace elements (e.g., Th and U) are intimately related to the soil characteristics and its mineral lattice structure and are mostly controlled by silicate and aluminosilicate minerals (Churchman and Lowe, 2012). The abundances of major elements, such as Si, K, and Al-rich phases, were predominantly associated to quartz, feldspar, and clays, whereas Fe and Ti were presumably bound to pyrite, hematite, titanite, and rutile in soils (Churchman and Lowe, 2012). The K_2O/Al_2O_3 ratios (mean: 0.16, range: 0.09–0.30) for the measured soils suggest the predominance of clays (K_2O/Al_2O_3: 0–0.30) rather than feldspars (0.3–0.9) or illites (0.28) (Cox et al., 1995). However, the K_2O/Na_2O ratio (mean: 6.6, range: 2.6–18.6) demonstrated probable occurrences of feldspars (Nesbitt and Markovics, 1980; Roser and Korsch, 1986; Carvalho et al., 2011). Furthermore, the SiO_2/Al_2O_3 ratio (mean: 5.5, range: 3.4–8.1) in investigated soils was significantly greater than that for kaolinite (1.18) (Roser and Korsch, 1986), indicating the relatively high proportions of quartz (Table 1). The Al_2O_3/TiO_2 values (mean: 15.5, range: 2.0–29.8) for the studied soil samples were relatively higher than the mafic (3–8) and lower than those of felsic sources but are comparable to those of intermediate source rocks (8–21) (Hayashi et al., 1997). Thus, the samples were presumably derived from felsic to intermediate igneous rock provenance (e.g., granitic source) (Begum et al., 2021b).

Considering the demonstration of Nesbitt and Young (1982), the chemical index of alteration (CIA = $[(Al_2O_3)/(CaO + Na_2O + K_2O + Al_2O_3)] \times 100\%$) were calculated for the studied soil samples, with the values ranging from 68.1% to 86.3% and having a mean of 80.6%. Thus, in terms of CIA value, the analyzed soil samples were highly weathered (Nesbitt and Young, 1982). Secondary clays and clay-like phases (e.g., kaolinite) had a CIA value of nearly 100% (Fedo et al., 1995; Nesbitt and Young, 1982), whereas illite and smectite revealed CIA values of 75–85%. UCC had a mean CIA of 47% (McLennan et al., 1993). Hence, considering the CIA values of the above-mentioned geo-materials, inference of the mineralogical compositions of studied soil samples indicated that kaolinite can be the major component of clays. Earlier studies have identified that clays comprise illite (26.3%), kaolinite (73.7%) (Aftabuzzaman et al., 2013), and quartz, feldspar, illite,

Table 1
Major oxides (wt%), radionuclides (Bq.kg^{-1}), and calculated U and Th concentrations (μg.g^{-1}) in soil samples around the coal-based power plant were compared with those of other geo-materials.

	SiO_2	Al_2O_3	Fe_2O_3	TiO_2	Na_2O	K_2O	CaO	MgO	^{226}Ra	^{232}Th	^{40}K	U	Th	Th/U
Mean (n = 48)	65.8	12.7	3.6	0.91	0.34	2.0	0.54	0.44	80.6	104.4	508.1	6.5	25.7	4.2
SD (1σ)	4.3	2.7	1.2	0.50	0.15	0.36	0.48	0.37	16.3	28.4	90.8	1.3	7.0	1.5
RSD (%)	6.6	21.5	32.9	55.1	43.9	17.7	88.1	83.7	20.3	27.1	17.9	20.3	27.1	37
Median	65.7	12.4	3.6	0.85	0.31	2.0	0.31	0.33	81.8	103.7	498.9	6.6	25.5	3.9
Min	56.4	8.2	1.2	0.5	0.1	1.2	0.1	0.0	33.0	43.0	318.3	2.7	10.6	1.4
Max	78.9	18.6	6.8	4.1	1.1	2.9	1.8	1.7	118.0	182.0	743.4	9.6	44.8	8.6
Relevant geo-materials														
WS[a]	70.6	13.4	5.7	0.83	0.67	1.7	2.1	0.83	24.7	36.5	438.2	2	9	4.5
WSH[a]	59.3	16.6	6.9	0.77	0.80	2.95	2.2	2.7	45.7	48.7	766.9	3.7	12	3.2
Granites[a]	71.9	14.6	3.9	0.38	3.7	4.0	2.2	0.27	54.3	93.4	1045.4	4.4	23	5.2
Basalts[a]	51.3	16.6	8.0	1.5	2.6	1.0	9.4	7.5	5.3	6.5	259.8	0.43	1.6	3.7
UCC[b]	66.6	15.4	5.0	0.64	3.3	2.8	3.6	2.5	33.3	42.6	720	2.7	10.5	3.7

WS: world soil; WSH: world shale; UCC: upper continental crust; [a]Bowen (1979); [b]Rudnick and Gao (2014); granites (felsic source rock); basalts (mafic source rock).

kaolinite, monazite, rutile, zircon, biotite, tourmaline, garnet, ilmenite, kyanite, and sillimanite minerals (major, trace, and accessory) (Habib et al., 2019b) present in soils from the present investigated area.

3.2. Soil radioactivity

The summary of radioactivity concentrations in the measured samples in this work and affiliated hazard indices, e.g., Ra_{eq}, H_{in}, GAD_i, AED_T, and ELCR, was compared with the relevant literature data in

Table 2
Activity concentration of ^{226}Ra, ^{232}Th, and ^{40}K (Bq.kg^{-1}) in soils from this study were compared with those of other regions of Bangladesh and coal industries around the world along with their calculated radiological risk indices: Ra_{eq} (Bq.kg^{-1}), H_{in}, GAD_i, AED_T, and ELCR (Sv^{-1}).

Region	^{226}Ra	^{232}Th	^{40}K	Ra_{eq}	H_i	GAD_i	AED_T	ELCR (×10^{-3})	Reference
This work									
Mean (n = 24) A-horizon	72.32	122.31	516.16	286.97	0.97	157.09	0.23	0.56	
Mean (n = 24) B-horizon	89.28	87.91	473.74	251.46	0.92	138.64	0.21	0.50	This study
Overall mean (n = 48)	80.61	104.40	508.05	269.03	0.94	147.89	0.22	0.53	
Literature data									
Bangladesh (Rangpur)	87	140	1844	429.19	1.394	244.40	0.36	0.67	Hamid et al., 2002
Bangladesh (Rampal)	34.8	48.9	719	160.09	0.526	91.53	0.14	0.56	Khan et al., 2019b
Bangladesh (Chittagong)	35.9	65.5	272	150.51	0.503	82.34	0.12	0.63	Chowdhury et al., 1999
Bangladesh (Southern)	42	81	833	221.97	0.713	125.17	0.19	0.78	Chowdhury et al., 2006
Bangladesh (Chittagong)	61	79.68	856.9	240.44	0.784	135.86	0.20	0.66	Alam et al., 2013
Bangladesh (Dhaka)	33	55	574	155.85	0.510	87.89	0.13	0.47	Miah et al., 1998
Bangladesh (Cox's Bazar)	19	36.7	458.2	106.76	0.340	60.71	0.09	0.48	Alam et al., 1999
Overall (mean: Bangladesh)	44.7	72.40	793.9	209.3	0.686	118.3	0.18	0.50	
Global data									
Xitulvye, China	49.4	63.5	396.3	170.72	0.59	94.49	0.14	0.58	Zhang, 2017
Kangal, Turkey	37	17	222	78.40	0.31	44.21	0.07	0.53	Gören et al., 2017
Serbia	50.7	48.6	560	169.58	0.58	95.77	0.14	0.59	Ćujić et al., 2015
Egypt	14.7	17.1	222	56.25	0.19	31.94	0.05	0.56	El-Mekawy et al., 2015
Mawan, South China	199	264	1216	670.15	2.35	367.86	0.55	0.54	Liu et al., 2015
Kapar, Malaysia	86.7	74.3	297.3	215.84	0.82	118.28	0.18	0.52	Amin et al., 2013
Raša, Croatia	55.2	0	365.2	264.74	0.95	145.91	0.22	0.54	Medunić et al., 2016
Megalopolis, Greece	45	32.5	337	117.42	0.44	65.93	0.10	0.64	Papaefthymiou et al., 2013
Velilla, Spain	38.7	42.9	445.3	134.34	0.47	75.60	0.11	0.52	Charro et al., 2013a
Douro, Portugal	53.105	46.3	845.1	184.36	0.64	105.96	0.16	0.54	Ribeiro et al., 2010
Agios Dimitrios,Greece	26.8	36.8	492.6	117.35	0.39	66.81	0.10	0.46	Karamanis et al., 2009
Nasik, India	37	69.6	396	138.37	0.48	78.58	0.12	0.54	Mishra, 2004
Kolaghat, India	111.4	140.2	350.7	338.9	1.22	183.87	0.27	0.49	Mandal and Sengupta, 2005
Baoji, China	32.1	49.8	720.6	158.80	0.52	90.79	0.13	0.59	Dai et al., 2007
Figueira, Brazil	133	39	233	206.71	0.92	114.31	0.17	0.50	Flues et al., 2002
Lodz, Poland	16.6	15.7	306.7	62.67	0.21	36.16	0.05	0.52	Bem et al., 2002
Ajka, Hungary	129	26.9	337	191.77	0.72	106.28	0.16	0.53	Papp et al., 2002
Germany	35	27	362	101.48	0.37	57.53	0.09	0.45	Roser and Korsch, 1986
Overall (mean: Global)	62.9	54.9	444.3	175.6	0.64	97.92	0.15	0.54	
Bangladesh	34 (21–43)		350 (130–610)						UNSCEAR, 2000
Critical values	370	259	810–925						Kabata-Pendias, 2010
Threshold values	33	45	420	≤370	≤1	≤60	≤0.50	≤0.29E-03	UNSCEAR, 2000
World soil	24.7	36.5	363.8	104.91	0.35	59.03	0.09	0.67	Bowen, 1979
Crust	33.3	42.6	720	149.66	0.494	86.04	0.13	0.56	Rudnick and Gao, 2014
Shale	45.7	48.7	766.9	175.59	0.598	100.56	0.15	0.63	Bowen, 1979

Table 2 along with their graphical distributions (Figs. 2–5). The average (ranges) radioactivity concentrations of ^{226}Ra, ^{232}Th, and ^{40}K for the top soils (A-horizon; depth: 0–15 cm) were 71.2 (54.2–99.0), 120.0 (76.6–182.0), and 525.8 (383.6–743.4) Bq.kg^{-1}, respectively. Meanwhile, for subsoils (B-horizon; depth: 15–30 cm), the mean (ranges) radioactivity concentrations were 90 (33–118), 88.9 (43.0–122.7), and 490.3 (318.3–682.0) Bq.kg^{-1}, respectively. The total radioactivity (Bq.kg^{-1}) of NORMs in the measured soils was 693, while 795.9 for UCC (Rudnick and Gao, 2014), 499.4 for WS, 861.3 for WSH, and 465 for the typical world value (UNSCEAR, 2010). The measured activity of NORMs were about 2.9–3.3, 1.8–2.1, 2.4–2.5, and 2.3–2.4 times higher compared with those of the typical median values for WS, WSH (Bowen, 1979), world recommended corresponding standards (UNSCEAR, 2010), and the background value for UCC, respectively, except for ^{40}K, whose relatively lower values were determined compared with the background values (Table 2). According to UNSCEAR (2000), the average (ranges) activity levels of ^{226}Ra and ^{40}K in Bangladesh soils are 34 (21–43) and 350 (130–610) Bq.kg^{-1}, respectively.

Earlier reported mean radioactivity concentrations of ^{226}Ra, ^{232}Th, and ^{40}K in the surface soils (within 3 km radius nearby Barapukuria CMPS) were 64, 103, and 494 Bq.kg^{-1}, respectively (Habib and Khan, 2021), which are relatively higher compared with those in the world recommended standard (UNSCEAR, 2010). However, the overall mean (ranges) radioactivity concentrations (n = 48) of ^{226}Ra, ^{232}Th, and ^{40}K were 80.6 (33.0–118.0), 104.4 (43.0–182.0), and 508.1 (318.3–743.4) Bq.kg^{-1}, respectively, for the analyzed samples in this study. The overall published mean (ranges) radioactivity concentrations of ^{226}Ra, ^{232}Th, and ^{40}K in soils around several power stations around the globe are 62.9 (14.7–199.0), 54.9 (15.7–264.0), and 444.3 (222–1216) Bq.kg^{-1}, respectively, which are considerably lower than the undesired higher radioactivity concentrations in this work (Table 2). The present specific activities of ^{226}Ra and ^{232}Th in soils around Barapukuria CMPS are unusually and relatively higher in the surveyed area than all other regions of Bangladesh, except for the northwestern (Rangpur) part of the country (Table 2). The radioactivity concentrations of ^{226}Ra of this work are 1.5–5.5 times higher than the other reported values for relevant soil samples around the world, except for Mawan (China: Liu et al., 2015), Kapar (Malaysia: Amin et al., 2013), Kolaghat (India: Mandal and Sengupta, 2005), Figueira (Brazil: Flues et al., 2002), and Ajka (Hungary: Papp et al., 2002) (Table 2). Meanwhile, the mean ^{232}Th activity concentrations of this work are 1.4–6.6 folds greater than the relevant reported global values, except for Mawan (China: Liu et al., 2015) and Kolaghat (India: Mandal and Sengupta, 2005) (Table 2). Concomitantly, the measured mean (n = 48) radioactivity concentrations of ^{226}Ra and ^{232}Th of this study are respectively 1.8 and 1.4 times higher than those results reported for soil samples from different parts of the country (Table 2). Furthermore, the ^{40}K radioactivity concentrations of this study are 1.0–2.3 times higher than the global values presented in Table 2, except for Serbia (Ćujić et al., 2015), Mawan (China: Liu et al., 2015), Douro (Portugal: Ribeiro et al., 2010), and Baoji (China: Dai et al., 2007). Meanwhile, the mean ^{40}K contents in Barapukuria CMPS soils are significantly lower than the mean values of the country (Table 2).

3.3. Potential incorporations of anthropogenic NORMs in the ambient pedosphere

In this study, the calculated mean (ranges) mass concentrations and mass ratios of U, Th, and Th/U, were 6.5 (2.7–9.6) ppm, 25.7 (10.6–44.8) ppm, and 4.2 (1.4–8.6), respectively. The mass concentrations of U and Th were evidently higher than those in WS, WSH, granites, basalts, and UCC (Bowen, 19799; Rudnick and Gao, 2014) (Table 1). The high Th/U ratios of this study were supposedly influenced by the weathering conditions of soils, which are an indication of dissolution and loss of U during geological processes (McLennan et al., 1993). A Th/U ratio > 4 denotes extreme weathering in provenance areas or sedimentary recycling, which is concomitant with the estimated CIA values (80.6%). Moreover, a high Th/U ratio value indicates the relatively high mobility of U compared with Th, which is expected to have high affinity with the accessory resistant minerals, such as monazite and zircon (Tamim et al., 2016). Therefore, U might have been washed away from the surroundings by alluvial–fluvial processes, leading to an elevated Th/U ratio. The calculated mean activity ratio of ^{232}Th/^{226}Ra for this study was 1.4, which is relatively higher than that of UCC (1.3), invoking an additional anthropogenic incorporation of ^{232}Th over ^{226}Ra.

The Al, UCC-normalized enrichment factors (EFs) of U and Th were 3.0 (range: 1.4–6.3) and 3.0 (range: 1.3–5.5), respectively, for the studied samples. An EF ≤ 2 can be assumed to be of geogenic source for an element, whereas EF > 2 is an indication of biogenic and/or anthropogenic origins (Reimann and de Caritat, 2005; Dragović et al., 2008; Sucharovà et al., 2012; Tume et al., 2018). The mean (range) ratios of radioactivity concentrations of ^{226}Ra, ^{232}Th, and ^{40}K between the surface soil and the corresponding sub-surface soil (A/B) were 0.83 (0.5–2.3), 1.44 (1.0–2.7), and 1.12 (0.7–2.3), respectively. NORM abundances in the surface soils were relatively higher in the southeastern part of the Barapukuria CMPS, whereas sub-surface soils showed opposite trends (Fig. 3), which are likely to be controlled by the wind-flow direction during winter. In terms of NORM ratios (surface/sub-surface), no distinct variations of NORM contents were observed between the surface and sub-surface soils, except for ^{232}Th, which can be explained by the variation in geochemical mobility, water solubility (rainwater), and redox conditions of the soil (Begum et al., 2021b; Khan et al., 2015, 2017, 2021a, 2021b). Furthermore, NORM concentrations in the studied area were relatively higher compared with those in the local and international reference data presented in Table 2, except for ^{40}K. Thus, given the EFs, the fractionation of ^{232}Th between surface and

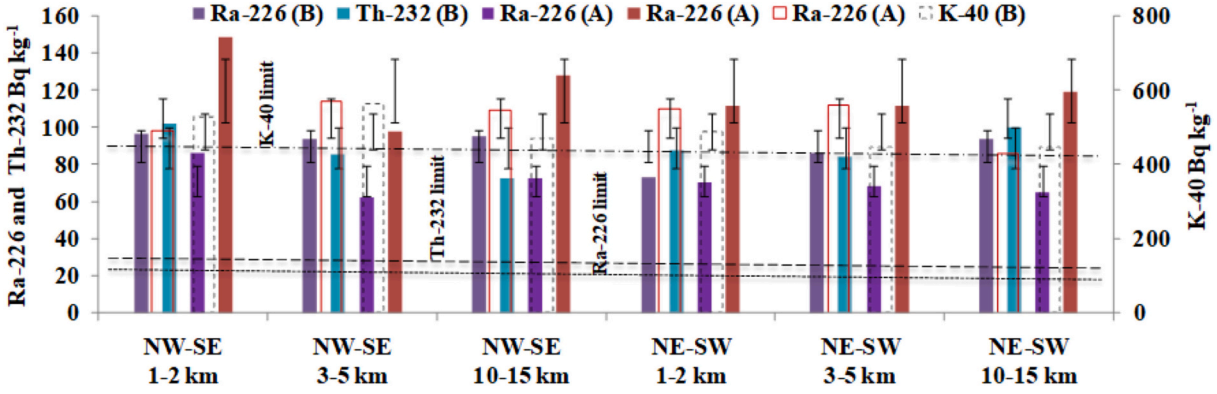

Fig. 2. Average activity of measured radionuclides in the samples collected at different depths (A-horizon, topsoil; B-horizon, sub-soil), directions, and distances. Uncertainty bars are also shown. Herein after, "A" and "B" indicate the surface layer and substrate soils, respectively.

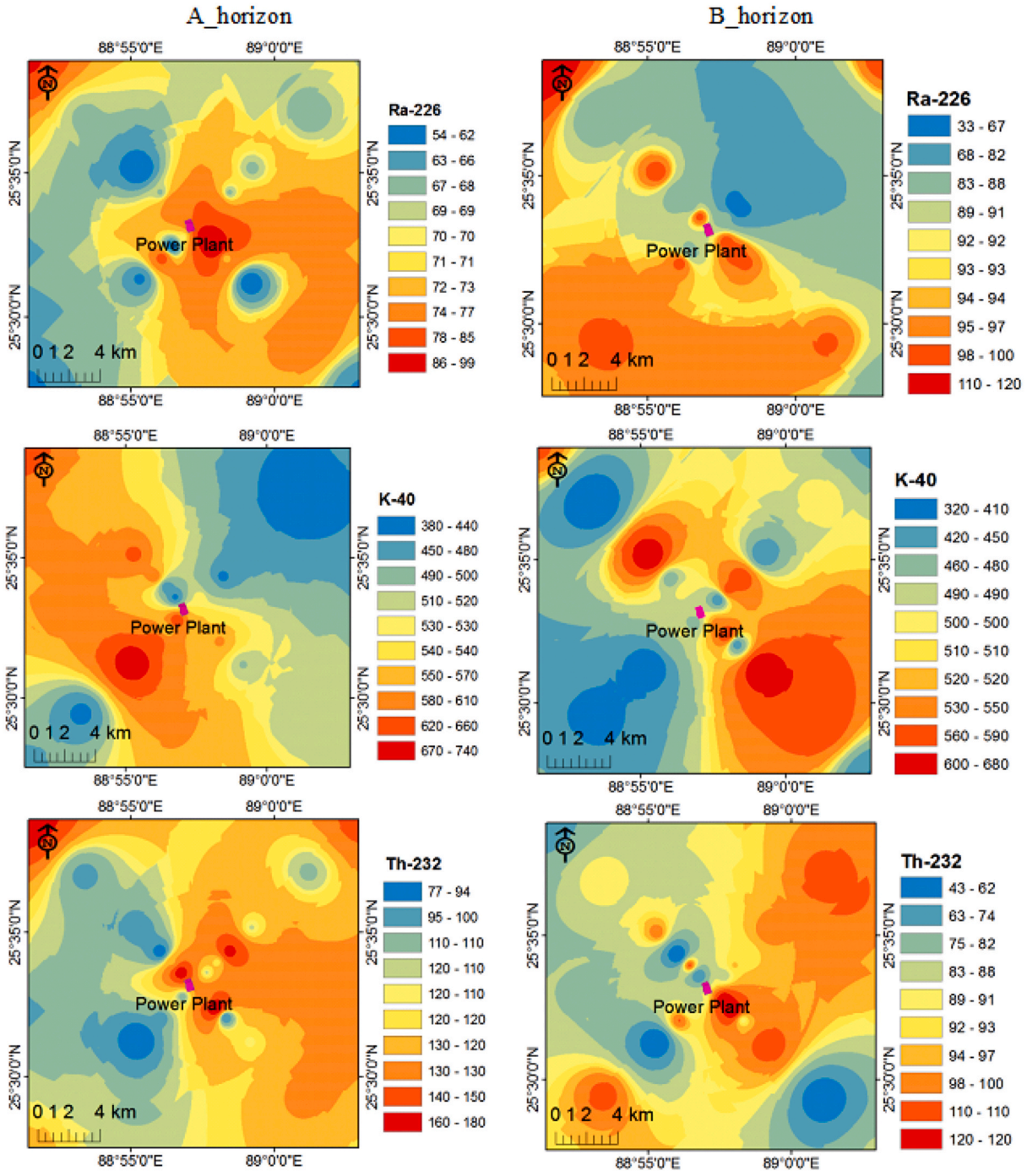

Fig. 3. Interpolated spatial variations of determined radionuclide activities (Bq.kg^{-1}) for both surface soils (A-horizon) and sub-surface soils (B-horizon) in the studied area.

sub-surface soils and comparisons with the literature data, the studied area receives anthropogenic NORMs from the coal-based power plant and coal mining activities.

3.4. Geochemical associations and co-occurrences

Geochemical associations and partitioning of NORMs in Barapukuria soils were evaluated by the correlation analysis in this study (Table S1). The strong correlation of Fe oxides (total) with Al_2O_3 ($r = 0.610$, $p < 0.01$) indicates the possible association of Fe-rich clays and other phases, such as Fe oxy-hydroxides, siderite, or hydrous clays and/or shales (Begum et al., 2021a, 2021b). These trends indicated that the abundances of Fe and K in the samples were appreciably influenced by Al-rich phases, such as clays, which are progressively diluted by quartz (Suresh et al., 2011). Moreover, the overall positive correlation (Table S1) between Al_2O_3 and K_2O ($r = 0.308$, $p < 0.05$) in the analyzed samples indicated the control of aluminosilicates residual clays, such as illite/smectite, kaolinite, and alkali feldspar, which are common in soils (Suresh et al., 2011). Clay minerals are great concentrators, carriers, and repositories for most of the elements in varying proportions given its large cation exchange capacity and very fine sized-grain and negatively charged surface (Habib et al., 2019b; Begum et al., 2021b; Khan et al., 2021a). In addition, the positive correlation between K_2O and Al_2O_3 implies that the concentrations of K-bearing minerals have a significant

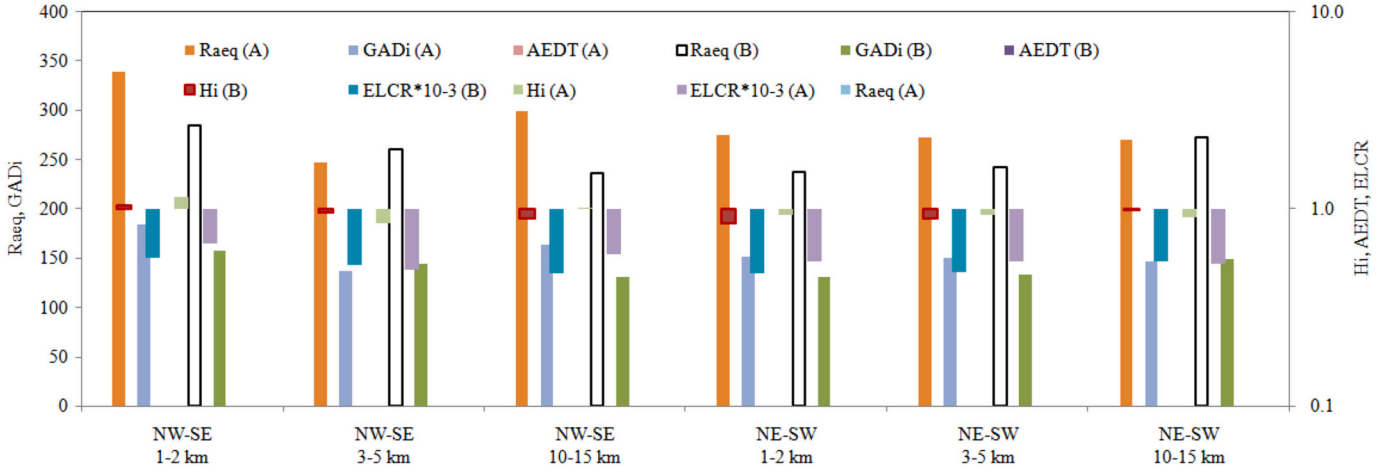

Fig. 4. Comparison of radiological hazard indices, such as Ra_{eq} ($Bq.kg^{-1}$), H_i, GAD_i ($nGy\ h^{-1}$), AED_T ($mSvy^{-1}$), and ELCR (sv^{-1}), in different directions of Barapukuria CMPS for A- and B-horizon soils.

influence on Al distribution and that the abundances of these elements are primarily controlled by the clay content (Suresh et al., 2011). Hence, Fe oxides (total), K_2O (along with ^{40}K), and Th (^{232}Th, $r = 0.410$, $p < 0.01$) showed a positive correlation with Al, which is likely due to their cooccurrence in nature and mutual dependence (Table S1). ^{232}Th was also positively correlated with ^{40}K ($r = 0.316$) in Barapukuria soils, which revealed their identical source of origin, e.g., coal-based industrial activities. Although, organic constituents can increase the solubility of Th, its mobility may be hindered due to the formation of almost insoluble precipitates and by adsorption on clays ($r_{Al\text{-}Th} = 0.41$) and organics ($r_{Th\text{-}OM} = 0.40$) (Barnett et al., 2000). The Th^{4+} subjects to extensive sorption by clays and organic substances at near-neutral pH (Ames et al., 1983), which leads to the immobilization of ^{232}Th and its fractionation between the surface and sub-surface soils. However, ^{226}Ra was not correlated with ^{232}Th and ^{40}K in the studied area, which is likely due to their different geochemical dynamics; the results are in good agreement with those of Pandit et al. (2020). Weak correlations among the NORMs were observed in this study. Thus, the coexistence of these NORMs is rare and likely governed by multiple factors, including re-condensation during coal burning, differential geochemical characteristics, aerodynamic dispersions of NORMs containing partials from CMPS, rainwater leaching, various physicochemical properties, etc.

3.5. Environmental fate and behavior of radioactive species in soils

The environmental fate and behavior of measured NORMs can be explained in terms of their relative geochemical mobility during diverse natural/geogenic processes. The computed RSD ($n = 48$) for ^{40}K and K_2O was ~18% (lowest among the NORMs), which indicates an almost homogeneous distribution with minor fractionations. K-bearing minerals, such as feldspars, clays, salts, and micas (fixed K), are relatively resistant to weathering (Nesbitt and Young, 1982; Kabata-Pendias, 2010), with ~95%–99% of this K being placed in the lattice of the associated minerals. However, during weathering (leaching) and alteration-dissolution these minerals potentially release K^+ ions, which are transferred to soil solutions and adsorbed on clays (Rachkova et al., 2010; Barnett et al., 2000). The high water solubility of K allows its high mobility during common geological processes. Thus, the almost homogeneous distribution of K (along with ^{40}K) in floodplain Barapukuria's soils can therefore be linked to the alluvial–fluvial processes that are concentrated during monsoonal heavy precipitation and flooding.

On the other hand, RSD (~27%, n = 48) for the ^{232}Th is the highest among the measured NORMs which reflect its relatively higher immobility. In geo-materials (e.g., soil and sediment), K along with Th are exclusively associated with aluminosilicates, namely, feldspar and clays, which are common in soils (Carvalho et al., 2011; Habib et al., 2019b). However, unlike K, Th is also partitioned in weather-resistant sysnsedimentary/syngenetic detrital particles/heavy minerals (e.g., monazite, zircon, fluorite, and apatite) (Khan et al., 2019a, 2019b, 2019c; Khan et al., 2021a, 2021b). Thus, Th migration usually occurs as a discrete mineral grain to the depository basin (syngenetic origin) (Parial et al., 2016). Hence, Th may not easily migrate in solutions from the source region due to its hydrolysis (as Th hydroxide) followed by on-site deposition (Khan et al., 2017, 2021a). As explained previously, ^{40}K distribution over the studied area was homogenized by flooding, surface run-off or by water logging during rainy season. However, in the case of Th, in aqueous systems, only Th^{4+} undergoes hydrolysis in aqueous solutions above pH 2–3. The Th^{4+} is subjected to extensive sorption by clays and organic acids at near-neutral pH (Kabata-Pendias, 2010). In near-neutral pH and alkaline soils, the precipitation of Th as a highly insoluble hydrated oxide phase and co-precipitation with hydrated ferric oxides ($r = 0.301$, $p < 0.05$) may, in addition to adsorption reactions, be important mechanisms for the removal of Th from solutions during flooding period in Barapukuria (Arogunjo et al., 2009). Given the sorption and precipitation reactions and slow solution rate of Th-bearing minerals, Th levels in natural waters are generally low (Greeman et al., 1990). Thus, migration of Th in the studied area is influenced by the formation of hydrated Th^{4+}, which is accountable for its immobilization over a wide range of soil pH. Furthermore, Th is unaffected by redox conditions and remains as insoluble Th^{4+}, which is the dominant species in soils. Hence, the water logging of the Barapukuria floodplain possesses trivial impact on the homogenization of the Th distribution. However, relatively lower RSD (~20%, $n = 48$) is observed for U ($\approx^{226}Ra$) in the studied site reflecting its relatively more water solubility and higher geochemical mobility than Th (Barnett et al., 2000; Rachkova et al., 2010; Siegel and Bryan, 2014). This condition is particularly true for weathering, in which K and U are well leached during the weatheringand alteration processes and easily transported in surficial media, but the highly stable Th is not (Barnett et al., 2000). The comparatively insoluble Th is concentrated in resistant minerals (e.g., monazite, zircon, and apatite), whereas U is redistributed in water sources (Harmsen and De Haan, 1980).

Usually, K, U, and Th contents and their corresponding activities are high in felsic granite rather than mafic basaltic source rocks (Pagel, 1982; Bowen, 1979; Kabata-Pendias, 2010; Yang et al., 2005), from where the studied soils might have originated. Habib et al. (2019b) demonstrated the presence of heavy minerals (e.g., monazite, rutile, zircon, biotite, tourmaline, garnet, ilmenite, etc.) in the studied area's soil samples, which contained high concentrations of Th and U. Thus, along with the anthropogenic source (such as coal-based industrial

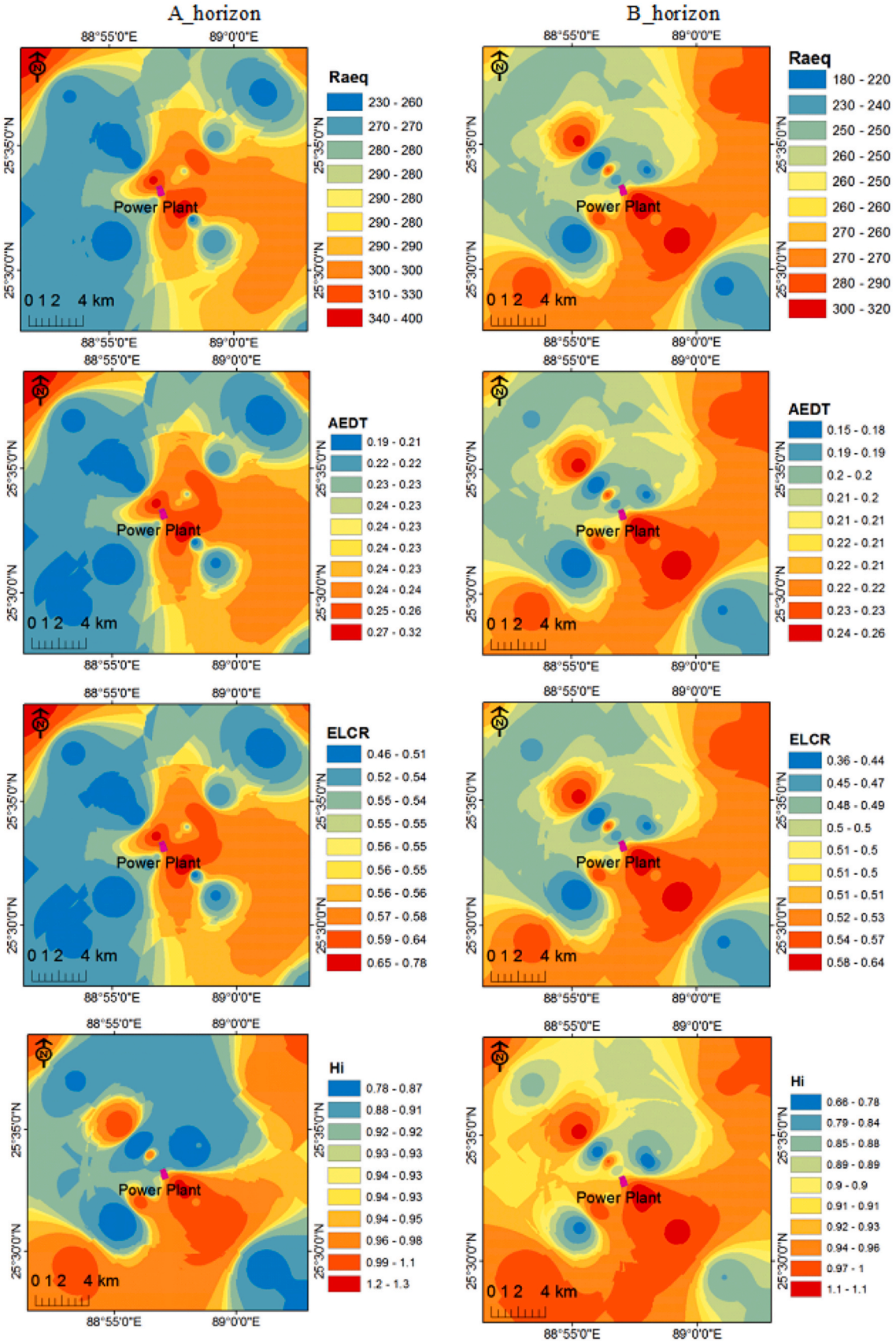

Fig. 5. Spatial distributions of radiological hazard indices, such as Ra_{eq} ($Bq.kg^{-1}$), H_i, GAD_i ($nGy\ h^{-1}$), AED_T ($mSvy^{-1}$), and ELCR (sv^{-1}) in and around the CMPS in Barapukuria.

activities), geochemical provenance plays a significant role in explaining the fate and distribution of NORMs. The retention of U by soils may occur due to certain effects of geochemical mechanisms (Rachkova et al., 2010; Khan et al., 2019a, 2019b; Khan et al., 2021a, 2021b). The processes of ion exchange, complexing, hydrolysis, and redox condition are responsible for U and Th fixation in soils (Arbuzov et al., 2011a, 2011b; Rachkova et al., 2010). Uranium, however, exists as the insoluble and stable U^{4+} in geological formations under reducing conditions, and it is relatively immobile because it forms sparingly soluble minerals (Chen et al., 2017). Moreover, the dissolved U^{3+} easily oxidizes to U^{4+} under most reducing conditions found in nature (Santos-Francés et al., 2018). However, under oxidizing conditions, insoluble U^{4+} is transformed into the comparatively soluble U^{6+} in soil solutions and water sources because UO_2^{+2} or as uranyl fluoride-, phosphate-, or carbonate-complexes can be mobilized easily in surficial processes and readily removed from soils, leading to the loss of U and simultaneously elevated Th/U (this study: 1.4 to 8.6) mass ratio in weathered products (Khan et al., 2015, 2018). Additionally, OM (this study: 0.5% to 9.5%) and clays are the most important sorbents of actinides (Rachkova et al., 2010), which can extract dissolved U from water sources and added slowly to soils over geologic time. Thus, the oxidizing environment triggered by rainwater logging distributed U (along with its daughter products) almost homogeneously among the surface and sub-surface soils of the studied area.

3.6. Radiological risk assessment

Maps of radioactivities, Ra_{eq}, H_i, GAD_i, AED_T, and ELCR of NORMs for the area were produced using geostatistical interpolation techniques and are presented in Figs. 3 and 5. The mean (n = 48) Ra_{eq} for the studied area is 269.0 (range: 182.0–398.1) $Bq.kg^{-1}$, which is lower than the threshold limit (370 $Bq.kg^{-1}$: UNSCEAR, 2000), except for the ~4.2% observed in sampling sites, where $Ra_{eq} > 370$ $Bq.kg^{-1}$. However, the mean H_i value of 0.94 (range: 0.66–1.33) is very close to the recommended limit (≤1), with ~23% of sampling sites possessing $H_i \geq 1$. Moreover, GAD_i ($nGy.h^{-1}$) values ranged from 101.1 to 216.2, with a mean value of 147.9, which are remarkably higher than the prescribed limit (60). On the other hand, all the estimated AED_T ($mSv.y^{-1}$) values (mean: 0.22, range: 0.15–0.32) is lower than the threshold limit (≤0.46). The estimated mean ELCR (Sv^{-1}) is 0.53×10^{-3} (range: 0.36×10^{-3} to 0.78×10^{-3}) (limit: $\leq 0.29 \times 10^{-3}$), which is significantly larger than the allowable limit. Hazard index values of GAD_i and ELCR crosses the limit of all sites in this study. The average soil activity of NORMs in soils at the studied area is within the recommended limits, except for GAD_i and ELCR whose values exceed the limit, although several unusual values have been noted. These findings are similar with those of global studies (Fig. 6). The average NORM activity of soils and the computed doses around CMPS are within the recommended limit for the world average for soil with several local variations.

This endeavor will encourage the concerned authorities to adopt proper measures to manage the produced wastes and tailings scientifically and sustainably to protect the environment and human health from potential radiological hazards, specifically the inhabitants residing around Barapukuria CMPS. In addition, caution should be provided concerning waste dumping because these disposal sites present a high specific activity and corresponding radiation dose consequences.

Environmental radioactivity and ionizing radiation exposure are also important phenomena of concern that may cause effects on human beings and the surroundings (Brugge and Buchner, 2011; Arbuzov et al., 2011a, 2011b; Bjørklund et al., 2017). Barapukuria soils are slightly

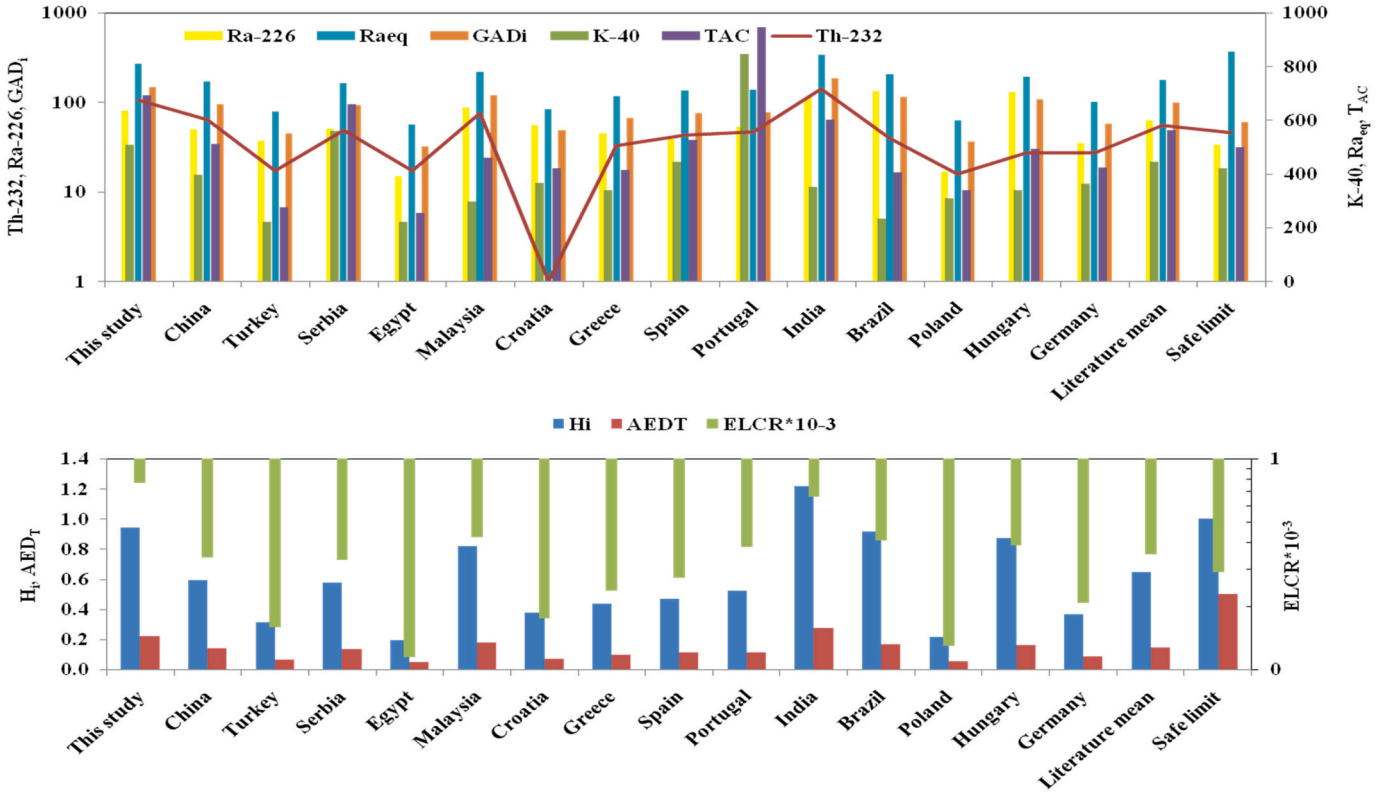

Fig. 6. Mean (n = 48) radioactivity concentrations and calculated radiological factors from this study were compared with worldwide literature data on coal industrial areas. The data were obtained from the following references: Xitulvye, China (Zhang, 2017); Kangal, Turkey (Gören et al., 2017); Serbia (Ćujić et al., 2015); Egypt (El-Mekawy et al., 2015); Kapar, Malaysia (Amin et al., 2013); Raša, Croatia (Medunić et al., 2016); Megalopolis, Greece (Papaefthymiou et al., 2013); Velilla, Spain (Charro et al., 2013a, 2013b); Douro, Portugal (Ribeiro et al., 2010); Nasik, India (Mishra, 2004); Figueira, Brazil (Flues et al., 2002); Lodz, Poland (Bem et al., 2002); Ajka, Hungary (Papp et al., 2002); Germany (Roser and Korsch, 1986); safe limit (UNSCEAR, 2000). Radiological indices: total specific activity (T_{AC}, $Bq.kg^{-1}$), Ra_{eq} ($Bq.kg^{-1}$), H_{in}, GAD_i ($nGy\ h^{-1}$), AED_T ($mSvy^{-1}$), and ELCR (sv^{-1}).

enriched with NORMs in comparison with the corresponding world average standards, posing a concern for potential radiation exposure of nearby living beings (Habib et al., 2019b). Environmental problems related to NORMs in feeding coals and associated combustion wastes may cause enhanced specific activities in soils, plants, and water around CMPS. Based on the earlier noted values, the mean activity levels of ^{226}Ra, ^{232}Th, and ^{40}K in soils are 63.6, 103.4, and 494.2 Bq.kg^{-1}, respectively, which are higher relative to world average (Habib et al., 2019b) although the country has no national or regional limit values for NORMs in soils. In northwestern region of Bangladesh, the levels of NORMs are substantially higher in soils in comparison with UNCEAR-recommended values (Hamid et al., 2002), in agreement with the current research findings. Similar observations involving high specific radioactivity in soils from coal utilization regions have been reported in global literatures (Table 2).

4. Conclusion

This study explored the potential geo-environmental pathways of NORM distributions in the ambient pedosphere in and around Barapukuria CMPS. The overall radioactivity concentrations in the studied soil samples were 1.3–3.5 times higher than the world average. The surface soil samples possessed relatively higher NORM contents compared with the sub-surface soils, where the ^{232}Th content was significantly fractionated between the surface and sub-surface soils. All the major oxides were depleted compared with those in crustal values, except for TiO_2. Concomitantly, the estimation of CIA (68.1–86.3%) revealed that the studied soil samples were highly weathered. The elevated abundances of NORMs compared with relevant local and international data along with the enriched NORMs in the surface soil (compared with the sub-surface soil) invoked the anthropogenic incorporation of NORMs to the geological background. This anthropogenic incorporation was then passed through several natural processes in the studied highly weathered pedosphere. Mineralogical phases dominated by clays with accessory heavy minerals, rainwater logging, redox condition, relative geochemical mobility, leaching, and differential solubility parameters of NORMs govern the NORM distribution. According to the interpolated spatial variations maps, ^{226}Ra and ^{232}Th are mostly partitioned in the eastern side when considering the surface soil only. However, only the aerodynamic dispersion of NORM-containing particulate matters from the power plant was not invoked because ^{40}K showed an opposite trend.

Radiological indices, e.g., Ra_{eq}, H_{in}, and AED_T values, were within the recommended threshold values, although specific sampling points surpassed the limits. However, the values of GAD_i and ELCR were significantly higher than the threshold values. Thus, long-term accumulations of anthropogenic NORMs in the local geology, their long half-lives, and life-long exposure to ionizing radiation can deteriorate the hazardous impacts of additional anthropogenic radioactivity. Thus, the outcomes of this study should be used to recommend proper steps in the management of technogenic wastes from power plants, which can be considered to have identical conditions globally.

Declaration of Competing Interest

The authors declare that they have no known competing financial interests or personal relationships that could have appeared to influence the work reported in this paper.

Acknowledgements

This research was supported by Prince of Songkla University under the Postdoctoral Fellowship Program. Authors would also like to greatly acknowledge the authority of the Geological Survey of Bangladesh for all other forms of support for this study.

Appendix A. Supplementary data

Supplementary data to this article can be found online at https://doi.org/10.1016/j.chemgeo.2022.120865.

References

Aftabuzzaman, M., Kabir, S., Islam, M.K., Alam, M.S., 2013. Clay mineralogy of the pleistocene soil horizon in Barind Tract, Bangladesh. J. Geol. Soc. India 81 (5), 677–684. https://doi.org/10.1007/s12594-013-0089-4.

Ahsan, M.A., Satter, F., Siddique, M.A.B., Akbor, M.A., Shamim, A., Shajahan, M., Khan, R., 2019. Chemical and physicochemical characterization of effluents from the tanning and textile industries in Bangladesh with multivariate statistical approach. Environ. Monit. Assess. https://doi.org/10.1007/s10661-019-7654-2.

Aközcan, S., Külahcı, F., Mercan, Y., 2018. A suggestion to radiological hazards characterization of 226Ra, 232Th, 40K and 137Cs: spatial distribution modelling. J. Hazard. Mater. 353, 476–489.

Alam, M.N., Chowdhury, M.I., Kamal, M., Ghose, S., Islam, M.N., Mustafa, M.N., Miah, M.M.H., Ansary, M.M., 1999. The 226Ra, 232Th and 40K activities in beach sand minerals and beach soils of Cox's Bazar, Bangladesh. J. Environ. Radioact. 46 (2), 243–250.

Alam, M.K., Chakraborty, S.R., Rahman, A.K.M.R., Deb, A.K., Kamal, M., Chowdhury, M. I., Uddin, M.S., 2013. Measurement of physiochemical parameters and determination of the level of radiological threat to the population associated with the Karnaphuli River sediment containing municipal and industrial wastes of Chittagong city in Bangladesh. Radiat. Prot. Dosim. 153 (3), 316–327.

Alazemi, N., Bajoga, A.D., Bradley, D.A., Regan, P.H., Shams, H., 2016. Soil radioactivity levels, radiological maps and risk assessment for the state of Kuwait. Chemosphere 154, 55–62. https://doi.org/10.1016/j.chemosphere.2016.03.057.

Ames, L.L., McGarrah, J.E., Walker, B.A., 1983. Sorption of uranium and radium by biotite, muscovite, and phlogopite. Clay Clay Miner. 31 (5), 343–351.

Amin, Y.M., Khandaker, M.U., Shyen, A.K.S., Mahat, R.H., Nor, R.M., Bradley, D.A., 2013. Radionuclide emissions from a coal-fired power plant. Appl. Radiat. Isot. 80, 109–116.

Arbuzov, S.I., Volostnov, A., Rikhvanov, L.P., Mezhibor, A.M., Ilenok, S.S., 2011a. Geochemistry of radioactive elements (U, Th) in coal and peat of northern Asia (Siberia, Russian Far East, Kazakhstan, and Mongolia). Int. J. Coal Geol. 86 (4), 318–328. https://doi.org/10.1016/j.coal.2011.03.005.

Arbuzov, S.I., Volostnov, A., Rikhvanov, L.P., Mezhibor, A.M., Ilenok, S.S., 2011b. Geochemistry of radioactive elements (U, Th) in coal and peat of northern Asia (Siberia, Russian Far East, Kazakhstan, and Mongolia). Int. J. Coal Geol. 86 (4), 318–328. https://doi.org/10.1016/j.coal.2011.03.005.

Arogunjo, A.M., Höllriegl, V., Giussani, A., Leopold, K., Gerstmann, U., Veronese, I., Oeh, U., 2009. Uranium and thorium in soils, mineral sands, water and food samples in a tin mining area in Nigeria with elevated activity. J. Environ. Radioact. 100 (3), 232–240.

ASTM C 998–83 (American Society for Testing and Materials), 1983. Standard Method for Sampling Surface Soil for Radionuclides, Annual Book of ASTM Standards Method C 998–83, Vol. 11.03. ASTM, Philadelphia, p. 512.

Baeza, A., Corbacho, J.A., Guillén, J., Salas, A., Mora, J.C., Robles, B., Cancio, D., 2012. Enhancement of natural radionuclides in the surroundings of the four largest coal-fired power plants in Spain. J. Environ. Monit. 14 (3), 1064–1072.

Barnett, M.O., Jardine, P.M., Brooks, S.C., Selim, H.M., 2000. Adsorption and transport of uranium (VI) in subsurface media. Soil Sci. Soc. Am. J. 64 (3), 908–917.

Begum, M., Khan, R., Hossain, S.M., Al Mamun, S.M.M.A., 2021a. Redistributions of NORMs in and around a gas-field (Shabazpur, Bangladesh): radiological risks assessment. J. Radioanal. Nucl. Chem. https://doi.org/10.1007/s10967-021-08107-x.

Begum, M., Khan, R., Roy, D.K., Habib, M.A., Rashid, M.B., Naher, K., Islam, M.A., Tamim, U., Das, S.C., Mamun, S.M.M.A., Hossain, S.M., 2021b. Geochemical characterization of Miocene core sediments from Shahbazpur gas-wells (Bangladesh) in terms of elemental abundances by instrumental neutron activation analysis. J. Radioanal. Nucl. Chem. https://doi.org/10.1007/s10967-021-07770-4.

Bem, H., Wieczorkowski, P., Budzanowski, M., 2002. Evaluation of technologically enhanced natural radiation near the coal-fired power plants in the Lodz region of Poland. J. Environ. Radioact. 61 (2), 191–201.

Beretka, J., Mathew, P.J., 1985. Natural radioactivity of Australian building materials, industrial wastes and by-products. Health Phys. 48 (1), 87–95.

Bjørklund, G., Christophersen, O.A., Chirumbolo, S., Selinus, O., Aaseth, J., 2017. Recent aspects of uranium toxicology in medical geology. Environ. Res. 156, 526–533.

Bowen, H.J.M., 1979. Environmental Chemistry of the Elements. Academic Press, London, New York.

Brugge, D., Buchner, V., 2011. Health effects of uranium: new research findings. Rev. Environ. Health 26 (4), 231–249.

Bunzl, K., Hötzl, H., Rosner, G., Winkler, R., 1984. Spatial distribution of radionuclides in soil around a coal-fired power plant: 210Pb, 210Po, 226Ra, 232Th, 40K emitted with the fly ash and 137Cs from the worldwide weapon testing fallout. Sci. Total Environ. 38, 15–31.

Carvalho, C., Anjos, R.M., Veiga, R., Macario, K., 2011. Application of radiometric analysis in the study of provenance and transport processes of Brazilian coastal sediments. J. Environ. Radioact. 102 (2), 185–192.

Çayır, A., Belivermiş, M., Kılıç, Ö., Coşkun, M., Coşkun, M., 2012. Heavy metal and radionuclide levels in soil around Afsin-Elbistan coal-fired thermal power plants, Turkey. Environ. Earth Sci. 67 (4), 1183–1190.

Charro, E., Pardo, R., Peña, V., 2013a. Statistical analysis of the spatial distribution of radionuclides in soils around a coal-fired power plant in Spain. J. Environ. Radioact. 124, 84–92.
Charro, E., Pardo, R., Peña, 2013b. Chemometric interpretation of vertical profiles of radionuclides in soils near a Spanish coal-fired power plant. Chemosphere 90 (2), 488–496.
Chen, J., Chen, P., Yao, D., Huang, W., Tang, S., Wang, K., Liu, W., Hu, Y., Li, Q., Wang, R., 2017. Geochemistry of uranium in Chinese coals and the emission inventory of coal-fired power plants in China. Int. Geol. Rev. 60 (5–6), 621–637.
Chowdhury, M.I., Alam, M.N., Hazari, S.K.S., 1999. Distribution of radionuclides in the river sediments and coastal soils of Chittagong, Bangladesh and evaluation of the radiation hazard. Appl. Radiat. Isot. 51 (6), 747–755.
Chowdhury, M.I., Kamal, M., Alam, M.N., Yeasmin, S., Mostafa, M.N., 2006. Distribution of naturally occurring radionuclides in soils of the southern districts of Bangladesh. Radiat. Prot. Dosim. 118 (1), 126–130.
Churchman, G.J., Lowe, D.J., 2012. Alteration, formation, and occurrence of minerals in soils. In: Huang, P.M., Li, Y., Sumner, M.E. (Eds.), Handbook of Soil Science. 2nd edition. Vol. 1: Properties and Processes. CRC press (Taylor and Francis), Boca Raton, FL, pp. 1–72.
Cox, R., Lowe, D.R., Cullers, R.L., 1995. The influence of sediment recycling and basement composition on evolution of mudrock chemistry in the southwestern United States. Geochim. Cosmochim. Acta 59 (14), 2919–2940.
Ćujić, M., Dragović, S., Đorđević, M., Dragović, R., Gajić, B., Miljanić, Š., 2015. Radionuclides in the soil around the largest coal-fired power plant in Serbia: radiological hazard, relationship with soil characteristics and spatial distribution. Environ. Sci. Pollut. Res. 22 (13), 10317–10330.
Ćujić, M., Dragović, S., Đorđević, M., Dragović, R., Gajić, B., 2016. Environmental assessment of heavy metals around the largest coal fired power plant in Serbia. CATENA 139, 44–52.
Dai, L., Wei, H., Wang, L., 2007. Spatial distribution and risk assessment of radionuclides in soils around a coal-fired power plant: a case study from the city of Baoji, China. Environ. Res. 104 (2), 201–208. https://doi.org/10.1016/j.envres.2006.11.005.
Dhingra, M., Kumar, M., Mehra, R., Sharma, N., 2020. Assessment of primordial radionuclide contents in soil samples and of impact of coal-based thermal power plant: a study in Tarn Taran district in Punjab, India. Radiat. Prot. Environ. 43 (1), 49.
Dragović, S., Mihailović, N., Gajić, B., 2008. Heavy metals in soils: distribution, relationship with soil characteristics and radionuclides and multivariate assessment of contamination sources. Chemosphere 72 (3), 491–495.
Dragović, S., Ćujić, M., Slavković-Beškoski, L., Gajić, B., Bajat, B., Kilibarda, M., Onjia, A., 2013. Trace element distribution in surface soils from a coal burning power production area: a case study from the largest power plant site in Serbia. Catena 104, 288–296.
Duong, V.H., Nguyen, T.D., Kocsis, E., Csordas, A., Hegedus, M., Kovacs, T., 2021. Transfer of radionuclides from soil to Acacia auriculiformis trees in high radioactive background areas in North Vietnam. J. Environ. Radioact. 229, 106530.
El-Mekawy, A.F., Badran, H.M., Seddeek, M.K., Sharshar, T., Elnimr, T., 2015. Assessment of elemental and NROM/TENORM hazard potential from non-nuclear industries in North Sinai, Egypt. Environ. Monit. Assess. 187 (9), 1–21.
Fedo, C.M., Wayne Nesbitt, H., Young, G.M., 1995. Unraveling the effects of potassium metasomatism in sedimentary rocks and paleosols, with implications for paleoweathering conditions and provenance. Geology 23 (10), 921–924.
Flues, M., Moraes, V., Mazzilli, B.P., 2002. The influence of a coal-fired power plant operation on radionuclide concentrations in soil. J. Environ. Radioact. 63 (3), 285–294.
Galhardi, J.A., García-Tenorio, R., Bonotto, D.M., Francés, I.D., Motta, J.G., 2017. Natural radionuclides in plants, soils and sediments affected by U-rich coal mining activities in Brazil. J. Environ. Radioact. 177, 37–47. https://doi.org/10.1016/j.jenvrad.2017.06.001.
Gören, E., Turhan, Ş., Kurnaz, A., Garad, A.M.K., Duran, C., Uğur, F.A., Yeğingil, Z., 2017. Environmental evaluation of natural radioactivity in soil near a lignite-burning power plant in Turkey. Appl. Radiat. Isot. 129, 13–18. https://doi.org/10.1016/j.apradiso.2017.07.059.
Goto, A., Tatsumi, Y., 1994. Quantitative analysis of rock samples by an X-ray fluorescence spectrometer (I). Rigaku J. 11, 40–59.
Goto, A., Tatsumi, Y., 1996. Quantitative analysis of rock samples by an X-ray fluorescence spectrometer (II). Rigaku J. 13, 20–38.
Greeman, D.J., Rose, A.W., Jester, W.A., 1990. Form and behavior of radium, uranium, and thorium in Central Pennsylvania soils derived from dolomite. Geophys. Res. Lett. 17 (6), 833–836.
Guagliardi, I., Rovella, N., Apollaro, C., Bloise, A., De Rosa, R., Scarciglia, F., Buttafuoco, G., 2016. Effects of source rocks, soil features and climate on natural gamma radioactivity in the Crati valley (Calabria, Southern Italy). Chemosphere 150, 97–108. https://doi.org/10.1016/j.chemosphere.2016.02.011.
Habib, M.A., Khan, R., 2021. Environmental impacts of coal-mining and coal-fired power-plant activities in a developing country with global context. In: Spatial Modeling and Assessment of Environmental Contaminants (Chapter 24), Environmental Challenges and Solutions. Switzerland AG, Springer Nature. https://doi.org/10.1007/978-3-030-63422-3_24.
Habib, M.A., Basuki, T., Miyashita, S., Bekelesi, W., Nakashima, S., Techato, K., Khan, R., Majlis, A.B.K., Phoungthong, K., 2019a. Assessment of natural radioactivity in coals and coal combustion residues from a coal-based thermoelectric plant in Bangladesh: implications for radiological health hazards. Environ. Monit. Assess. 191, 27. https://doi.org/10.1007/s10661-018-7160-y.
Habib, M.A., Basuki, T., Miyashita, S., Bekelesi, W., Nakashima, S., Phoungthong, K., Khan, R., Rashid, M.B., Islam, A.R.M.T., Techato, K., 2019b. Distribution of naturally occurring radionuclides in soil around a coal-based power plant and their potential radiological risk assessment. Radiochim. Acta 107 (3), 243–259. https://doi.org/10.1515/ract-2018-3044.
Habib, M.A., Islam, A.R.M.T., Bodrud-Doza, M., Mukta, F.A., Khan, R., Siddique, M.A.B., Phoungthong, K., Techato, K., 2020. Simultaneous appraisals of pathway and probable health risk associated with trace metals contamination in groundwater from Barapukuria coal basin, Bangladesh. Chemosphere 242. https://doi.org/10.1016/j.chemosphere.2019.125183.
Hamid, B.N., Chowdhury, M.I., Alam, M.N., Islam, M.N., 2002. Study of natural radionuclide concentrations in an area of elevated radiation background in the Northern districts of Bangladesh. Radiat. Prot. Dosim. 98 (2), 227–230.
Harmsen, K., De Haan, F.A.M., 1980. Occurrence and behaviour of uranium and thorium in soil and water. NJAS Wageningen J. Life Sci. 28 (1), 40–62.
Hasan, M.N., Siddique, M.A.B., Reza, A.H.M.S., Khan, R., Akbor, M.A., Elius, I.B., Hasan, A.B., Hasan, M., 2022. Vulnerability assessment of seawater intrusion in coastal aquifers of southern Bangladesh: Water quality appraisals. Environ. Nanotechnol. Monitor. Manag. 16, 100498. https://doi.org/10.1016/j.enmm.2021.100498.
Hayashi, K.I., Fujisawa, H., Holland, H.D., Ohmoto, H., 1997. Geochemistry of~ 1.9 Ga sedimentary rocks from northeastern Labrador, Canada. Geochim. Cosmochim. Acta 61 (19), 4115–4137.
IAEA (International Atomic Energy Agency), 2004. Soil Sampling for Environmental Contaminants. IAEA-TECDOC-1415, Vienna, Austria.
ICRP (International Commission on Radiological Protection), 1990. Recommendations of the International Commission on Radiological Protection, 212 (1–3); Publication 60. UK Pergamon Press, Oxford.
Kabata-Pendias, A., 2010. Trace Elements in Soils and Plants, Fourth edition. CRC Press. Taylor and Francis, Florida.
Karamanis, D., Ioannides, K., Stamoulis, K., 2009. Environmental assessment of natural radionuclides and heavy metals in waters discharged from a lignite-fired power plant. Fuel 88 (10), 2046–2052. https://doi.org/10.1016/j.fuel.2009.02.032.
Khan, R., Shirai, N., Ebihara, M., 2015. Chemical characteristics of R chondrites in the light of REE, Th, U and P abundances. Earth Planet. Sci. Lett. 422, 18–27. https://doi.org/10.1016/j.epsl.2015.04.008.
Khan, R., Rouf, M.A., Das, S., Tamim, U., Naher, K., Podder, J., Hossain, S.M., 2017. Spatial and multi-layered assessment of heavy metals in the sand of Cox's-Bazar beach of Bangladesh. Reg. Stud. Mar. Sci. 16, 171–180. https://doi.org/10.1016/j.rsma.2017.09.003.
Khan, R., Parvez, M.S., Tamim, U., Das, S., Islam, M.A., Naher, K., Khan, M.H.R., Nahid, F., Hossain, S.M., 2018. Assessment of rare earth elements, Th and U profile of a site for a potential coal-based power plant by instrumental neutron activation analysis. Radiochim. Acta 106 (6), 515–524. https://doi.org/10.1515/ract-2017-2867.
Khan, R., Das, S., Kabir, S., Habib, M.A., Naher, K., Islam, M.A., Tamim, U., Rahman, A.K.M.R., Deb, A.K., Hossain, S.M., 2019a. Evaluation of the elemental distribution in soil samples collected from ship-breaking areas and an adjacent island. J. Environ. Chem. Eng. 7 https://doi.org/10.1016/j.jece.2019.103189.
Khan, R., Parvez, M.S., Jolly, Y.N., Haydar, M.A., Alam, M.F., Khatun, M.A., Sarker, M.M.R., Habib, M.A., Tamim, U., Das, S., Sultana, S., Islam, M.A., Naher, K., Paul, D., Akter, S., Khan, M.H.R., Nahid, F., Huque, R., Rajib, M., Hossain, S.M., 2019b. Elemental abundances, natural radioactivity and physicochemical records of a southern part of Bangladesh: implication for assessing the environmental geochemistry. Environ. Nanotechnol. Monitor. Manag. 12 https://doi.org/10.1016/j.enmm.2019.100225.
Khan, R., Ghosal, S., Sengupta, D., Tamim, U., Hossain, S.M., Agrahari, S., 2019c. Studies on heavy mineral placers from eastern coast of Odisha, India by instrumental neutron activation analysis. J. Radioanal. Nucl. Chem. 319 (1), 471–484. https://doi.org/10.1007/s10967-018-6250-1.
Khan, R., Islam, H.M.T., Islam, A.R.M.T., 2021a. Mechanism of elevated radioactivity in a freshwater basin: radiochemical characterization, provenance and associated hazards. Chemosphere 264 (1). https://doi.org/10.1016/j.chemosphere.2020.128459.
Khan, R., Mohanty, S., Sengupta, D., 2021b. Studying the elemental distribution in the core sediments of Podampata, Eastern coast of Odisha, India: potentiality of rare earth elements and Th exploration. Arab. J. Geosci. 14, 81. https://doi.org/10.1007/s12517-020-06371-x.
L'Annunziata, M.F., 2003. Handbook of Radioactivity Analysis (2003), 2nd ed. Academic Press, San Diego. 1273p.
Liu, G., Luo, Q., Ding, M., Feng, J., 2015. Natural radionuclides in soil near a coal-fired power plant in the high background radiation area, South China. Environ. Monit. Assess. 187 (6), 356.
Lu, X., Liu, W., Zhao, C., Chen, C., 2013. Environmental assessment of heavy metal and natural radioactivity in soil around a coal-fired power plant in China. J. Radioanal. Nucl. Chem. 295 (3), 1845–1854.
Mandal, A., Sengupta, D., 2005. Radionuclide and trace element contamination around Kolaghat Thermal Power Station, West Bengal–environmental implications. Curr. Sci. 617–624.
McLennan, S.M., Hemming, S., McDaniel, D.K., Hanson, G.N., 1993. Geochemical approaches to sedimentation provenance and tectonics. In: Johnsson, M.J., Basu, A. (Eds.), Processes Controlling the Composition of Clastic Sediment, vol. 284. Geological Society of America Special Paper, pp. 21–40.
Medunić, G., Ahel, M., Mihalić, I.B., Srček, V.G., Kopjar, N., Fiket, Ž., Bituh, T., Mikac, I., 2016. Toxic airborne S, PAH, and trace element legacy of the superhigh-organic-sulphur Raša coal combustion: cytotoxicity and genotoxicity assessment of soil and ash. Sci. Total Environ. 566, 306–319.

Miah, F.K., Roy, S., Touchiduzzaman, M., Alam, B., 1998. Distribution of radionuclides in soil samples in and around Dhaka city. Appl. Radiat. Isot. 49 (1–2), 133–137.
Mishra, U.C.Ā., 2004. Environmental impact of coal industry and thermal power plants in India. J. Environ. Radioact. 72 (1–2), 35–40. https://doi.org/10.1016/S0265-931X(03)00183-8.
Nesbitt, H.W., Markovics, G., 1980. Chemical processes affecting alkalis and alkaline earths during continental weathering. Geochim. Cosmochim. Acta 44 (11), 1659–1666.
Nesbitt, H.W., Young, G.M., 1982. Early Proterozoic climates and plate motions inferred from major element chemistry of lutites. Nature 299, 715–717.
Noli, F., Tsamos, P., Stoulos, S., 2017. Spatial and seasonal variation of radionuclides in soils and waters near a coal-fired power plant of Northern Greece: environmental dose assessment. J. Radioanal. Nucl. Chem. 311 (1), 331–338.
Pagel, M., 1982. The mineralogy and geochemistry of uranium, thorium, and rare-earth elements in two radioactive granites of the Vosges, France. Mineral. Mag. 46 (339), 149–161.
Pandit, P., Mangala, P., Saini, A., Bangotra, P., Kumar, V., Mehra, R., Ghosh, D., 2020. Radiological and pollution risk assessments of terrestrial radionuclides and heavy metals in a mineralized zone of the Siwalik region (India). Chemosphere 254, 126857.
Papaefthymiou, H.V., Manousakas, M., Fouskas, A., Siavalas, G., 2013. Spatial and vertical distribution and risk assessment of natural radionuclides in soils surrounding the lignite-fired power plants in megalopolis basin, Greece. Radiat. Prot. Dosim. 156 (1), 49–58. https://doi.org/10.1093/rpd/nct037.
Papp, Z., Dezső, Z., Daroczy, S., 2002. Significant radioactive contamination of soil around a coal-fired thermal power plant. J. Environ. Radioact. 59 (2), 191–205.
Parial, K., Guin, R., Agrahari, S., Sengupta, D., 2016. Monitoring of radionuclide migration around Kolaghat thermal power plant, West Bengal, India. J. Radioanal. Nucl. Chem. 307 (1), 533–539. https://doi.org/10.1007/s10967-015-4152-z.
Rachkova, N.G., Shuktomova, I.I., Taskaev, A.I., 2010. The state of natural radionuclides of uranium, radium, and thorium in soils. Eur. Soil Sci. 43 (6), 651–658.
Rahman, M.A., Siddique, M.A.B., Khan, R., Reza, A.H.M.S., Khan, A.H.A.N., Akbor, M.A., Islam, M.S., Hasan, A.B., Hasan, M.I., Elius, I.B., 2022. Mechanism of arsenic enrichment and mobilization in groundwater from southeastern Bangladesh: water quality and preliminary health risks assessment. Chemosphere. https://doi.org/10.1016/j.chemosphere.2022.133556.
Reimann, C., de Caritat, P., 2005. Distinguishing between natural and anthropogenic sources for elements in the environment: regional geochemical surveys versus enrichment factors. Sci. Total Environ. 337 (1–3), 91–107.
Ribeiro, J., Ferreira da Silva, E., Li, Z., Ward, C., Flores, D., 2010. Petrographic, mineralogical and geochemical characterization of the Serrinha coal waste pile (Douro Coalfield, Portugal) and the potential environmental impacts on soil, sediments and surface waters. Int. J. Coal Geol. 83 (4), 456–466. https://doi.org/10.1016/j.coal.2010.06.006.
Ribeiro, F.C.A., Silva, J.I.R., Lima, E.S.A., do Amaral Sobrinho, N.M.B., Perez, D.V., Lauria, D.C., 2018. Natural radioactivity in soils of the state of Rio de Janeiro (Brazil): radiological characterization and relationships to geological formation, soil types and soil properties. J. Environ. Radioact. 182, 34–43.
Roser, B.P., Korsch, R.J., 1986. Determination of tectonic setting of sandstone-mudstone suites using SiO2 content and K2O/Na2O ratio. J. Geol. 94, 635–650.
Rosner, G., Bunzl, K., Hötzl, H., Winkler, R., 1984. Low level measurements of natural radionuclides in soil samples around a coal-fired power plant. Nucl. Instr. Methods Phys. Res. 223 (2–3), 585–589.
Rudnick, R.L., Gao, S., 2014. Composition of the continental crust. In: Holland, H.D., Turekian, K.K. (Eds.), The Crust (ed. R.L. Rudnick), Vol. 4, Treatise on Geochemistry, 2nd edition. Elsevier-Pergamon, Oxford, pp. 1–51.
Santos-Francés, F., Pacheco, E.G., Martinez-Grana, A., Rojo, P.A., Zarza, C.Á., Sánchez, A. G., 2018. Concentration of uranium in the soils of the west of Spain. Environ. Pollut. 236, 1–11.
Sengupta, D., Agrahari, S., 2017. Heavy metal and radionuclide contaminant migration in the vicinity of thermal power plants: Monitoring, remediation, and utilization. In: Modelling Trends in Solid and Hazardous Waste Management. Springer, Singapore, pp. 15–33.
Siegel, M.D., Bryan, C.R., 2014. Radioactivity, geochemistry, and health (chapter 11.6). In: Holland, H.D., Turekian, K.K. (Eds.), Treatise on Geochemistry, 2nd ed. Elsevier, Amsterdam, Netherlands; Oxford, England; Waltham, Massachusetts, pp. 191–256.
Skoko, B., Marović, G., Babić, D., Šoštarić, M., Jukić, M., 2017. Plant uptake of 238U, 235U, 232Th, 226Ra, 210Pb and 40K from a coal ash and slag disposal site and control soil under field conditions: a preliminary study. J. Environ. Radioact. 172, 113–121.
Sucharovà, J., Suchara, I., Hola, M., Marikova, S., Reimann, C., Boyd, R., Filzmoser, P., Englmaier, P., 2012. Top−/bottom-soil ratios and enrichment factors: what do they really show? Appl. Geochem. 27 (1), 138–145.
Suhana, J., Rashid, M., 2016. Naturally occurring radionuclides in particulate emission from a coal fired power plant: a potential contamination? J. Environ. Chem. Eng. 4 (4), 4904–4910. https://doi.org/10.1016/j.jece.2016.07.015.
Suresh, G., Ramasamy, V., Meenakshisundaram, V., Venkatachalapathy, R., Ponnusamy, V., 2011. A relationship between the natural radioactivity and mineralogical composition of the Ponnaiyar river sediments, India. J. Environ. Radioact. 102 (4), 370–377.
Tamim, U., Khan, R., Jolly, Y.N., Fatema, K., Das, S., Naher, K., Islam, M.A., Islam, S.M. A., Hossain, S.M., 2016. Elemental distribution of metals in urban river sediments near an industrial effluent source. Chemosphere 155, 509–518. https://doi.org/10.1016/j.chemosphere.2016.04.099.
Tanić, M.N., Janković-Mandić, L., Gajić, B.A., Dakovic, M.Z., Dragović, S.D., Bacic, G.G., 2016. Natural radionuclides in soil profiles surrounding the largest coal-fired power plant in Serbia. Nucl. Technol. Radiat. Protect. 31 (3), 247–259.
Tanić, M.N., Ćujić, M.R., Gajić, B.A., Daković, M.Z., Dragović, S.D., 2018. Content of the potentially harmful elements in soil around the major coal-fired power plant in Serbia: relation to soil characteristics, evaluation of spatial distribution and source apportionment. Environ. Earth Sci. 77 (1), 1–14.
Tsikritzis, L.I., 2004. Chemometry of the distribution and origin of 226Ra, 232Th, 40K and 137Cs in the soil near the lignite fired plants of West Macedonia (Greece). J. Radioanal. Nucl. Chem. 2004 (261), 215–220.
Tume, P., González, E., King, R.W., Cuitiño, L., Roca, N., Bech, J., 2018. Distinguishing between natural and anthropogenic sources for potentially toxic elements in urban soils of Talcahuano, Chile. J. Soils Sediments 18 (6), 2335–2349.
Turhan, Ş., 2020. Evaluation of agricultural soil radiotoxic element pollution around a lignite-burning thermal power plant. Radiochim. Acta 108 (1), 77–85.
Ugbede, F.O., Osahon, O.D., Akpolile, A.F., 2021. Natural radioactivity levels of 238U, 232Th and 40K and radiological risk assessment in paddy soil of Ezillo rice fields in Ebonyi State, Nigeria. Environ. Forensic 1–16.
UNSCEAR, 2000. Sources and effects of ionizing radiation. In: United Nations Scientific Committee on the Effects of Atomic Radiation. United Nations Publication, New York, USA (2000).
UNSCEAR, 2010. Sources and effects of ionizing radiation. In: United Nations Scientific Committee on the Effects of Atomic Radiation. United Nations Publication, New York, USA (2010).
Vuković, Ž., Mandić, M., Vuković, D., 1996. Natural radioactivity of ground waters and soil in the vicinity of the ash repository of the coal-fired power plant "Nikola Tesla" A—Obrenovac (Yugoslavia). J. Environ. Radioact. 33 (1), 41–48.
Yang, Y.X., Wu, X.M., Jiang, Z.Y., Wang, W.X., Lu, J.G., Lin, J., Wang, L.M., Hsia, Y.F., 2005. Radioactivity concentrations in soils of the Xiazhuang granite area, China. Appl. Radiat. Isot. 63 (2), 255–259.
Zhang, X., 2017. Radioactivity level of soil around a coal-fired thermal power plant of Northwest China. Int. J. Radiat. Res. 15 (3), 321–324.